



Research

Cite this article: Feo TJ, Field DJ, Prum RO. 2015 Barb geometry of asymmetrical feathers reveals a transitional morphology in the evolution of avian flight. *Proc. R. Soc. B* **282**: 20142864.
<http://dx.doi.org/10.1098/rspb.2014.2864>

Received: 20 November 2014
Accepted: 14 January 2015

Subject Areas:
evolution, palaeontology

Keywords:
avian flight, asymmetrical flight feather, theoretical morphospace, evolutionary transition, Paraves, *Archaeopteryx*

Author for correspondence:
Teresa J. Feo
e-mail: teresa.feo@yale.edu

Electronic supplementary material is available at <http://dx.doi.org/10.1098/rspb.2014.2864> or via <http://rspb.royalsocietypublishing.org>.

Barb geometry of asymmetrical feathers reveals a transitional morphology in the evolution of avian flight

Teresa J. Feo^{1,2}, Daniel J. Field^{3,4} and Richard O. Prum^{1,2}

¹Department of Ecology and Evolutionary Biology, Yale University, 21 Sachem Street, New Haven, CT 06511, USA

²Peabody Museum of Natural History, and ³Department of Geology and Geophysics, Yale University, New Haven, CT, USA

⁴Department of Vertebrate Zoology, Smithsonian National Museum of Natural History, Washington, DC, USA

TJF, 0000-0002-4189-8692; DJF, 0000-0002-1786-0352

The geometry of feather barbs (barb length and barb angle) determines feather vane asymmetry and vane rigidity, which are both critical to a feather's aerodynamic performance. Here, we describe the relationship between barb geometry and aerodynamic function across the evolutionary history of asymmetrical flight feathers, from Mesozoic taxa outside of modern avian diversity (*Microraptor*, *Archaeopteryx*, *Sapeornis*, *Confuciusornis* and the enantiornithine *Eopengornis*) to an extensive sample of modern birds. Contrary to previous assumptions, we find that barb angle is not related to vane-width asymmetry; instead barb angle varies with vane function, whereas barb length variation determines vane asymmetry. We demonstrate that barb geometry significantly differs among functionally distinct portions of flight feather vanes, and that cutting-edge leading vanes occupy a distinct region of morphospace characterized by small barb angles. This cutting-edge vane morphology is ubiquitous across a phylogenetically and functionally diverse sample of modern birds and Mesozoic stem birds, revealing a fundamental aerodynamic adaptation that has persisted from the Late Jurassic. However, in Mesozoic taxa stemward of Ornithurae and Enantiornithes, trailing vane barb geometry is distinctly different from that of modern birds. In both modern birds and enantiornithines, trailing vanes have larger barb angles than in comparatively stemward taxa like *Archaeopteryx*, which exhibit small trailing vane barb angles. This discovery reveals a previously unrecognized evolutionary transition in flight feather morphology, which has important implications for the flight capacity of early feathered theropods such as *Archaeopteryx* and *Microraptor*. Our findings suggest that the fully modern avian flight feather, and possibly a modern capacity for powered flight, evolved crownward of *Confuciusornis*, long after the origin of asymmetrical flight feathers, and much later than previously recognized.

1. Introduction

Understanding the evolution of complex functional traits, like the avian wing, remains a fundamental challenge in biology. Aerial locomotion evolved in the lineage leading to modern birds and was accompanied by the acquisition of a suite of associated anatomical and physiological adaptations [1]. Among the most prominent characters associated with flight in birds are the elongated, asymmetrical primary feathers (primaries) of the wing in which the trailing vane is wider than the leading vane. Primaries create the aerodynamic surface of the outer wing and collectively function as an aerofoil to generate lift during flight [2]. The branched, pennaceous flight feathers of modern birds evolved from the tubular integumentary appendages of early theropod dinosaurs such as *Sinosauropteryx*, and were subsequently co-opted for an aerodynamic function with the evolution of asymmetrical pennaceous feathers in Paraves, i.e. theropods that are more closely related to modern birds than to

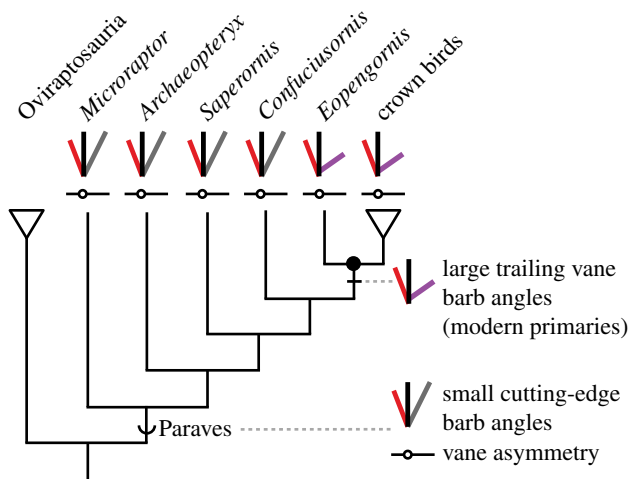


Figure 1. Simplified phylogeny of Paraves, and the evolution of asymmetrical flight feather barb geometry. Flight feather branching geometry of measured Mesozoic stem birds and crown birds showing the proposed evolutionary history of asymmetrical flight feather barb geometry. Small barb angles in cutting-edge leading vanes that function as the edge of an aerofoil (red) arose early in the evolutionary history of asymmetrical flight feathers, whereas large barb angles in trailing vanes that overlap other feathers to form the main surface of an aerofoil (purple) arose on the internode subtending the most recent common ancestor of Enantiornithes and Ornithurae (solid black circle). (Online version in colour.)

oviraptorosaurs (figure 1) [3–5]. The asymmetrical primaries of Mesozoic taxa such as *Microraptor* and *Archaeopteryx* (collectively referred to here as stem birds) provide *prima facie* evidence for the evolution of some form of aerial theropod locomotion by the Jurassic [6]. However, the extent to which the asymmetrical feathers of stem birds are anatomically modern, and thus functionally equivalent to those of living volant birds, is a topic of active research [6–14].

Two important aerodynamic adaptations of primaries are vane-width asymmetry and vane-shape emargination (figure 2a). In all extant flying birds, vane-width asymmetry (generated by a relatively narrow leading vane and a wider trailing vane) effectively shifts the rachis closer to the leading edge of the feather. Positioning the rachis within 35% of the chord length behind the leading edge allows a flight feather to dynamically maintain feather stability, or pitch in airflow [7,9]. In many birds, primary vane emarginations (i.e. sharp changes in the width of a vane along its length) result in separated feather tips when the wing is spread (figure 2a), which reduces induced drag on the wing [15,16]. The separated tips of emarginated feathers act as independent aerofoils during flight [15,16]. The aerodynamic function of flight feather vanes varies within and among feathers, so we partition the flight feather vane into four basic categories based on their hypothesized functions (figure 2a). *Cutting-edge leading vanes* function as the cutting edge of an aerofoil during flight, *free-edge trailing vanes* function as the unsupported trailing edge of an aerofoil during flight, and *supported leading vanes* and *supported trailing vanes* overlap with, and are supported by, neighbouring feathers to create a continuous surface of the wing.

Both vane-width asymmetry and vane-shape emargination are caused by variation in vane width within a feather. Each feather vane is composed of a series of branches called barbs attached to the rachis, and each barb consists of a series of

smaller branches called barbules attached to a central ramus (figure 2b). Vane width is determined by barb length and barb angle with respect to the rachis, which are each controlled by different developmental processes [2,17]. During the tubular development of a feather, radial position of the new barb locus determines barb length asymmetry, whereas differential barb expansion as the feather unfurls from the sheath determines barb angle asymmetry [17,18].

The developmental capacity to independently vary barb angle and barb length allows for a theoretical vane-width morphospace that is highly redundant [17,18]; any given vane width can be produced by many different combinations of barb length and barb angle (figure 2c). Thus, two feathers with the same vane widths could vary extensively in barb geometry. However, smaller barb angles also increase a vane's rigidity and response to the aerodynamic forces experienced in flight [2,19]. As a result, two feathers with the same vane width, but with different barb geometries, may also vary in their response to aerodynamic forces due to differences in their barb angles.

The developmental independence of barb angle and barb length creates an opportunity for the independent evolution of vane rigidity and overall feather shape. Feather stability (i.e. pitch control) derived from vane asymmetry, and drag reduction derived from vane emarginations, may be controlled independently of vane rigidity derived from barb angle. Consequently, superficial observations of vane asymmetry among modern and Mesozoic flight feathers do not necessarily indicate similar aerodynamic capabilities or flight styles; rather, the relationship between barb length and barb angle must be understood to draw confident conclusions about the functional performance of flight feathers in the fossil record.

Both barb angle and barb length are known to vary in the primary feathers of extant birds, and it is generally assumed that variation in barb angle is responsible for vane-width asymmetry [2,17,19,20]. However, the relationship between barb geometry and the functional partitions of asymmetrical flight feather vanes has previously never been investigated. Here, we analysed the flight feathers of flying birds, flightless birds and Mesozoic stem birds to characterize the relationship between barb geometry and vane partitions across the evolutionary history of asymmetrical flight feathers, shedding new light on the macro-evolutionary origins of one of the most characteristic features of modern avian anatomy.

2. Material and methods

(a) Feather specimens

We analysed the outer primaries of 60 species of modern flying birds from 34 families representing a broad range of phylogenetic diversity, body masses and flight styles (electronic supplementary material, table S1). Loose feathers of modern birds (i.e. not attached to study skins) were imaged with an Epson Perfection V700 Scanner at 3200 dpi. To investigate how the loss of flight influences feather barb geometry, we measured barb angles from the outermost primaries of 22 species of secondarily flightless birds. These species were distributed across seven avian orders and represent at least seven independent losses of flight (electronic supplementary material, table S1). Outermost primaries of flightless species were attached to study skins and were photographed in front of a piece of white paper with a Nikon SLR camera fitted with a macro lens. Modern feathers

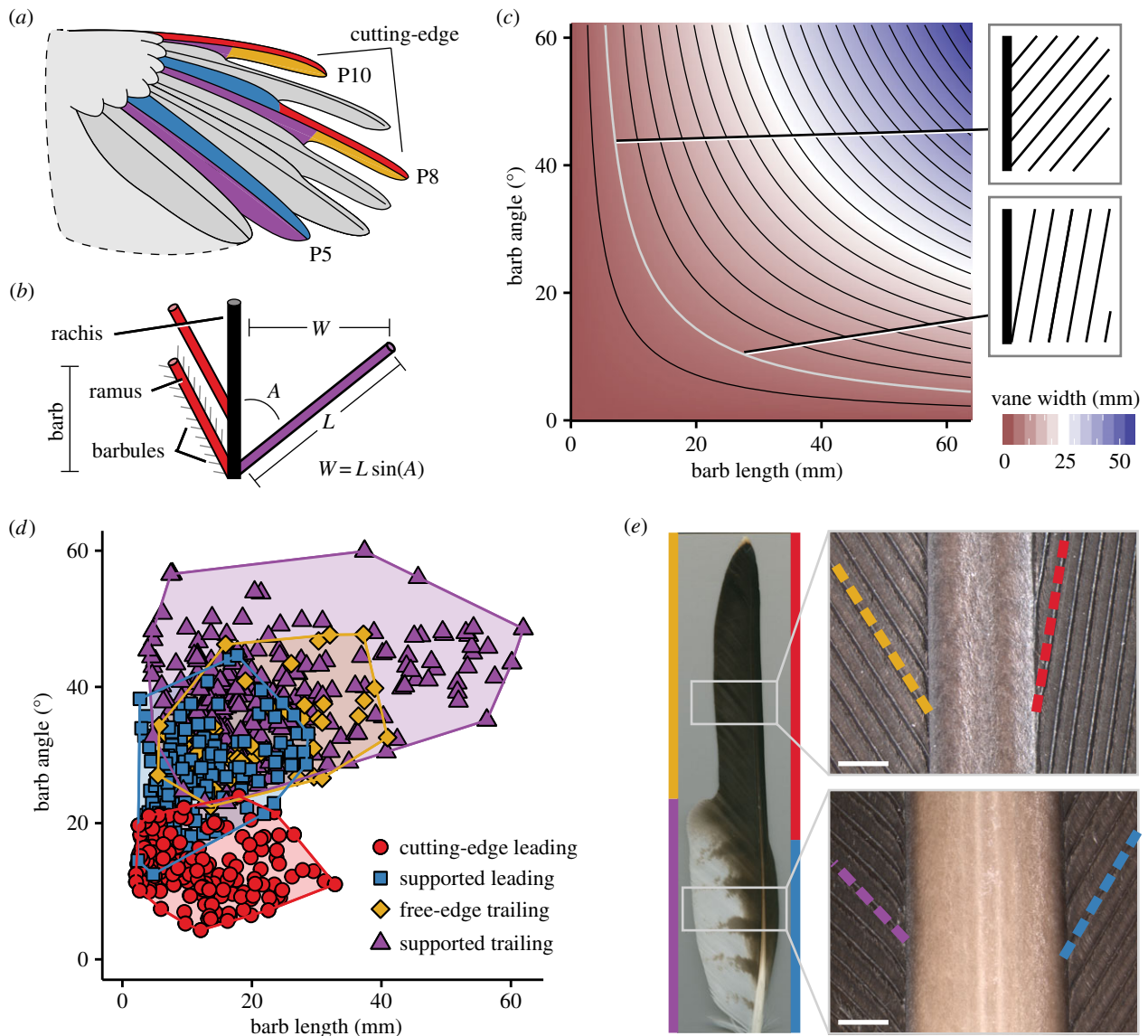


Figure 2. Flight feather morphology, theoretical vane-width morphospace and barb geometry of flying crown group birds. (a) Asymmetrical outer primary feathers of the wing with vane partitions identified by proposed aerodynamic functions: (red) cutting-edge leading vanes, (blue) supported leading vanes, (yellow) free-edge trailing vanes and (purple) supported trailing vanes. (b) Schematic of mature feather branch morphology; vane width (W) is dependent on barb length (L) and barb angle with respect to the rachis (A). (c) Theoretical morphospace of vane width (colour scale) based on barb geometry; different combinations of barb angle and barb length can produce feather vanes with the same width (grey contour line), but with qualitatively distinct barb geometries (insets). (d) Barb geometries of 60 extant flying bird species from 34 families. Cutting-edge leading vanes (red circles) are restricted to a distinct region of morphospace characterized by small barb angles. (e) Images of osprey, *Pandion haliaetus*, P8 detailing small barb angles in the cutting-edge portion of the leading vane, and larger angles throughout the rest of the feather. Scale bars, 1 mm. (Online version in colour.)

were obtained from the United States Fish and Wildlife Service Forensics Laboratory, Yale Peabody Museum of Natural History, American Museum of Natural History, University of California Berkeley Museum of Vertebrate Zoology and University of California Davis Museum of Wildlife and Fish Biology.

We measured outer primaries from *Archaeopteryx lithographica*, *Sapeornis chaoyangensis*, *Confuciusornis sanctus* and *Eopengornis martini*, as well as the outer hindwing feathers of *Microraptor gui* (electronic supplementary material, table S1). Feathers of Mesozoic taxa were studied from high-resolution digital photographs of prepared fossils. The Mesozoic specimens derive from a variety of fossil localities of varying ages and diagenetic histories, and have correspondingly been subjected to varying taphonomic regimes. However, none of the specimens exhibit any signs of taphonomic distortion that might influence barb measurements, such as evidence of unnatural overlapping or barb separation.

(b) Feather measurements

All measurements were made from digital images in IMAGEJ (<http://rsbweb.nih.gov/ij/>) with the OBJECTJ plugin (<http://simon.bio.uva.nl/objectj/>). For each modern flying species we measured three primaries from one adult individual: the outermost primary P10, P8 and P5 (or P9, 7, 4 in nine-primaried species). For each feather, we measured barb angle, barb length and vane width for leading and trailing vanes at 25% and 50% of total vane length from the tip of the feather. For each modern flightless species, we measured the trailing and leading vane of the outermost primary at 50% from the feather tip. For each Mesozoic species, we measured the outermost flight feather of the fore- or hindwings, as well as one or two additional outer primaries near the midpoint of each feather.

The presence and position from the tip of any vane emarginations were noted for each feather. Measurements taken from

the leading vanes of all P10, and any other leading vanes distal to an emargination, were categorized as cutting-edge vanes. Measurements taken from trailing vanes distal to an emargination were categorized as free-edge vanes. All remaining measurements were taken from vanes that overlap other feathers in a spread wing and were categorized as supported vanes. Barb and vane asymmetries were calculated as the difference between the trailing vane and leading vane (trailing–leading).

(c) Morphospace analyses

The theoretical morphospace of vane width is derived from equation (1) of Feo & Prum [17], in which vane width (W) is the distance between the rachis and the tip of a barb with length (L) and angle (A):

$$W = L \sin(A). \quad (2.1)$$

To compare barb geometries among different groups of feathers, we used measured values of barb angle and barb length to plot primaries into vane-width morphospace. Primaries were assessed for qualitative differences in barb geometry among different taxonomic and functional groups. The area of morphospace occupied by a given group of feathers was calculated as the minimum area of the convex hull surrounding all points in a group. The percentage of overlap between groups was calculated using the PBSmapping package in R [21]. Comparisons of morphospace occupancy were made for different taxonomic orders, different flight styles, different feather positions within the wing (P10, P8, P5), different positions along the length of feathers (25% and 50% from the feather tip), different vanes (trailing and leading), and different vane functional partitions (cutting-edge leading, supported leading, free-edge trailing and supported trailing).

(d) Statistical analyses

To account for non-independence of species, we analysed the dataset of 60 extant flying species measured 25% from the feather tip using phylogenetic generalized least squares (PGLS). Analyses used a majority rules consensus tree identified by MESQUITE [22] based on a sample of 100 trees sampled from the posterior distribution of Jetz *et al.* [23] (<http://www.birdtree.org>). We ran PGLS analyses in R [24] using the ape [25] and caper [26] software packages. Measurements were log transformed as needed to obtain a normal distribution. For each set of comparisons, each vane or feather was analysed separately, and the level of significance (α) was adjusted using a Bonferroni correction to account for multiple tests. Regressions between barb characters and vane width included vane type as a categorical variable, except for tests with the leading vane of P10 (because all vanes are a cutting edge), and tests with the trailing vane of P5 (because only one vane in our sample was a free-edge). Body mass data were obtained from Dunning [27]. Where Dunning provides data for both sexes, we used the mass of the sex of the bird from which we obtained feathers; when the sex of the bird was unknown, we averaged the male and female mass data provided by Dunning. Flight styles of extant flying birds follow the definitions presented by Bruderer *et al.* [28].

3. Results

(a) Modern flying birds

Within the flight feathers of modern birds, we found a similar range of barb geometries across different orders, different flight styles, different feather positions within the wing, and different positions along the length of feathers (electronic supplementary material, figure S1a–d). Conversely, leading and trailing vanes only partially overlapped in morphospace

owing to relatively larger angles in the trailing vane, and relatively smaller angles in the leading vane (electronic supplementary material, figure S1e). When classified by vane partition, free-edge trailing vanes, supported trailing vanes and supported leading vanes overlapped extensively with each other in morphospace due to their similar ranges of large barb angles (figure 2d). By contrast, cutting-edge leading vanes were restricted to a distinct region of morphospace characterized by small barb angles (less than 24°). Within an individual emarginated feather, the distinct differences in barb geometry of different vane partitions are readily apparent; small barb angles are present only along the cutting edge of the leading vane, whereas larger barb angles are present throughout the rest of the feather (figure 2e).

Developmental independence of barb length and barb angle theoretically creates the opportunity to regulate vane rigidity independently of feather asymmetry. In order to occupy redundant barb geometries within the vane-width morphospace (figure 2c), feathers must be able to independently modify barb angle and barb length. Using phylogenetic regression we found no significant relationship between barb length and barb angle within the leading and trailing vanes of feathers among the entire sample of modern birds, indicating that these two barb characters do vary independently of each other (electronic supplementary material, figure S2 and table S2).

Barb angle and barb length collectively determine vane width, and differences between leading and trailing vanes in one or both of these characters can lead to vane-width asymmetry [17,18]. Historically, barb angle variation has been assumed to be responsible for vane asymmetry in flight feathers [2,17,19,20]. We regressed barb angle and barb length against vane width to determine the relative contribution of each barb character to vane-width asymmetry. In contrast to previous assumptions, variation in barb angle was largely independent of vane width or vane-width asymmetry (figure 3a,b). We observed no significant correlations between barb angle and vane width within most feather vanes (figure 3a), except for a weak-positive relationship in the leading vane of P5 (electronic supplementary material, figure S3a and table S3). We also observed no significant relationships between barb angle asymmetry and vane-width asymmetry within most feathers (figure 3b), except for a weak-positive relationship in P10 (electronic supplementary material, figure S3b and table S4).

Variation in vane width, and vane-width asymmetry, were instead primarily driven by barb length. We discovered strong-positive relationships between barb length and vane width within the leading and trailing vanes of feathers, and strong-positive relationships between barb length asymmetry and vane-width asymmetry within feathers (figure 3c,d; electronic supplementary material, table S5, S6). Although allometry influences many aspects of avian functional anatomy [29], the relationship between barb length and vane width was found to be independent of body size (electronic supplementary material, figure S4a and table S7), as was barb angle (electronic supplementary material, figure S4b and table S8).

Small barb angles can contribute to vane rigidity—i.e. resistance to aerodynamic forces during flight [2,19]. We included vane edge as an additional categorical variable in the phylogenetic regressions to determine if barb geometry varied among different vane functions. Both barb angle and barb length significantly differed between cutting-edge and supported leading vane partitions, but not between trailing

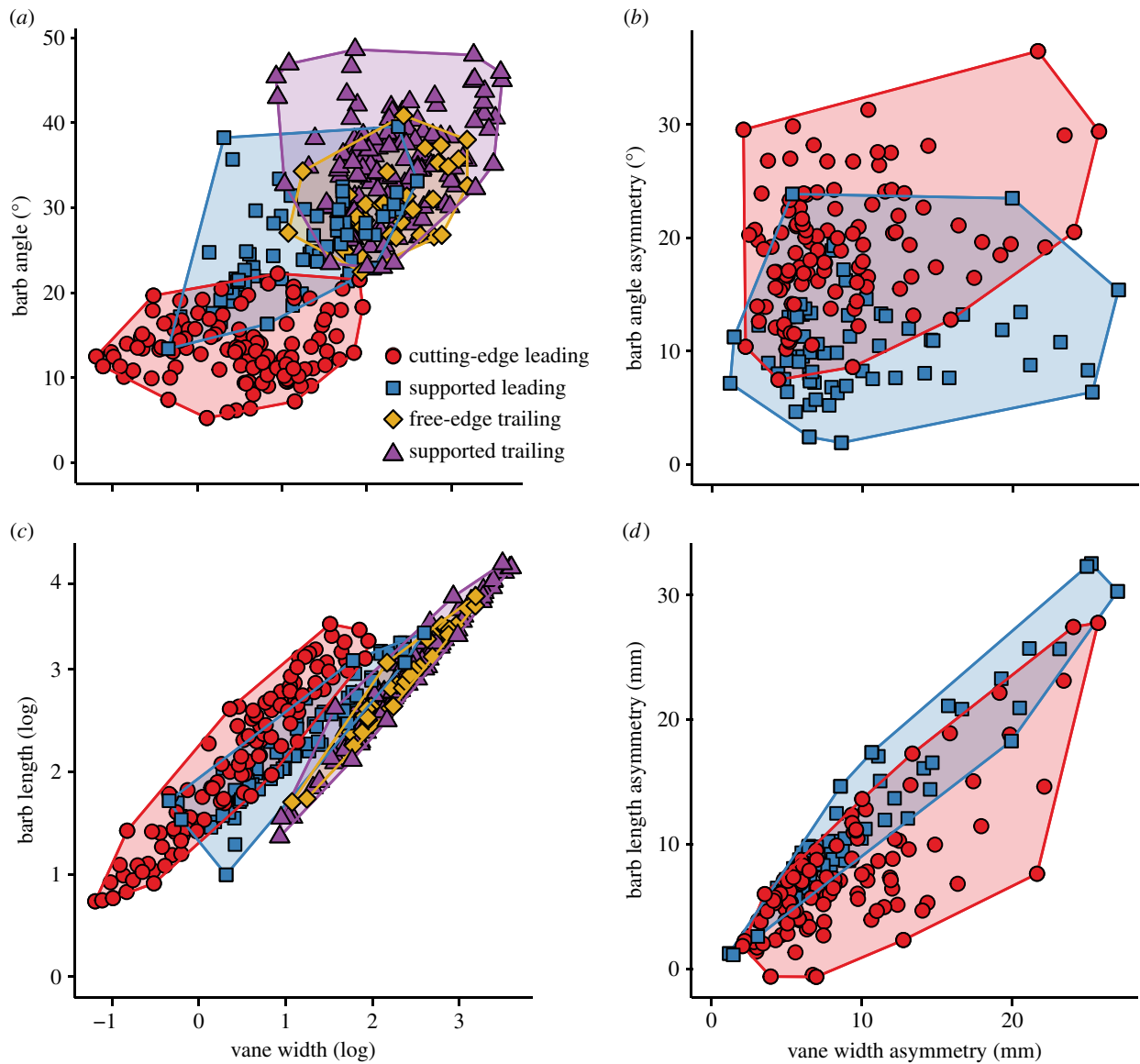


Figure 3. Bivariate plots of barb angle and barb length versus vane width of flying crown birds. (a) There is no significant relationship between barb angle and vane width across most feather vanes. (b) There is no significant correlation between barb angle asymmetry and vane-width asymmetry across most feathers. (c) Barb length significantly increases with increasing vane width across all feather vanes. (d) Barb length asymmetry significantly increases with increasing vane-width asymmetry across all feathers. Barb angles and barb length significantly differ between cutting-edge (red circles) and supported (blue squares) leading vanes, but do not differ between free-edge (yellow diamonds) and supported (purple triangles) trailing vanes. Data shown are combined from primaries 10, 8 and 5 measured 25% from tip. See the electronic supplementary material, tables S3–S6 for PGLS statistics. (Online version in colour.)

vane partitions (figure 3; electronic supplementary material, tables S3–S6). Cutting-edge leading vanes exhibited significantly smaller barb angles, and significantly longer barbs compared with supported leading vanes of the same width (figure 3, red circles versus blue squares). Conversely, free-edge and supported trailing vanes with similar vane widths did not significantly differ in their barb geometry (figure 3, yellow diamonds versus purple triangles).

(b) Modern flightless birds

Flying ability has been lost multiple times across crown birds, and many secondarily flightless species retain highly asymmetric primaries despite a release from active selection for aerodynamic performance [30,31]. Vane-width asymmetry was sufficient in all species to position the rachis within the 35% functional threshold for automatic pitch control, except for the flightless rail *Megacrex inepta* (figure 4a, orange circles). Most flightless species retained the small leading vane barb

angles and large trailing vane barb angles of their volant ancestors (figure 4b, orange versus red, and brown versus purple circles). In some species, such as the steamer ducks (*Tachyeres* sp.) and the great auk (*Pinguinus impennis*), these barb geometries may reflect natural selection for a hydrodynamic function during wing-propelled swimming [32]. Leading vane barb angles in *M. inepta*, *Porzana sandwichensis*, *Xenicus lyalli* and *Gallirallus australis* were relatively large and fell outside the range of cutting-edge barb angles in flying birds (figure 4b, labelled orange circles). Overall, the primaries of most flightless birds were indistinguishable from those of flying birds in terms of their vane asymmetry and barb geometry.

(c) Mesozoic stem birds

The outer fore- and hindwing feathers of many Mesozoic stem birds (figure 1) exhibit elongated asymmetrical feathers and have generally been assumed to be morphologically indistinguishable from modern flight feathers [6,9,14,33]. However,

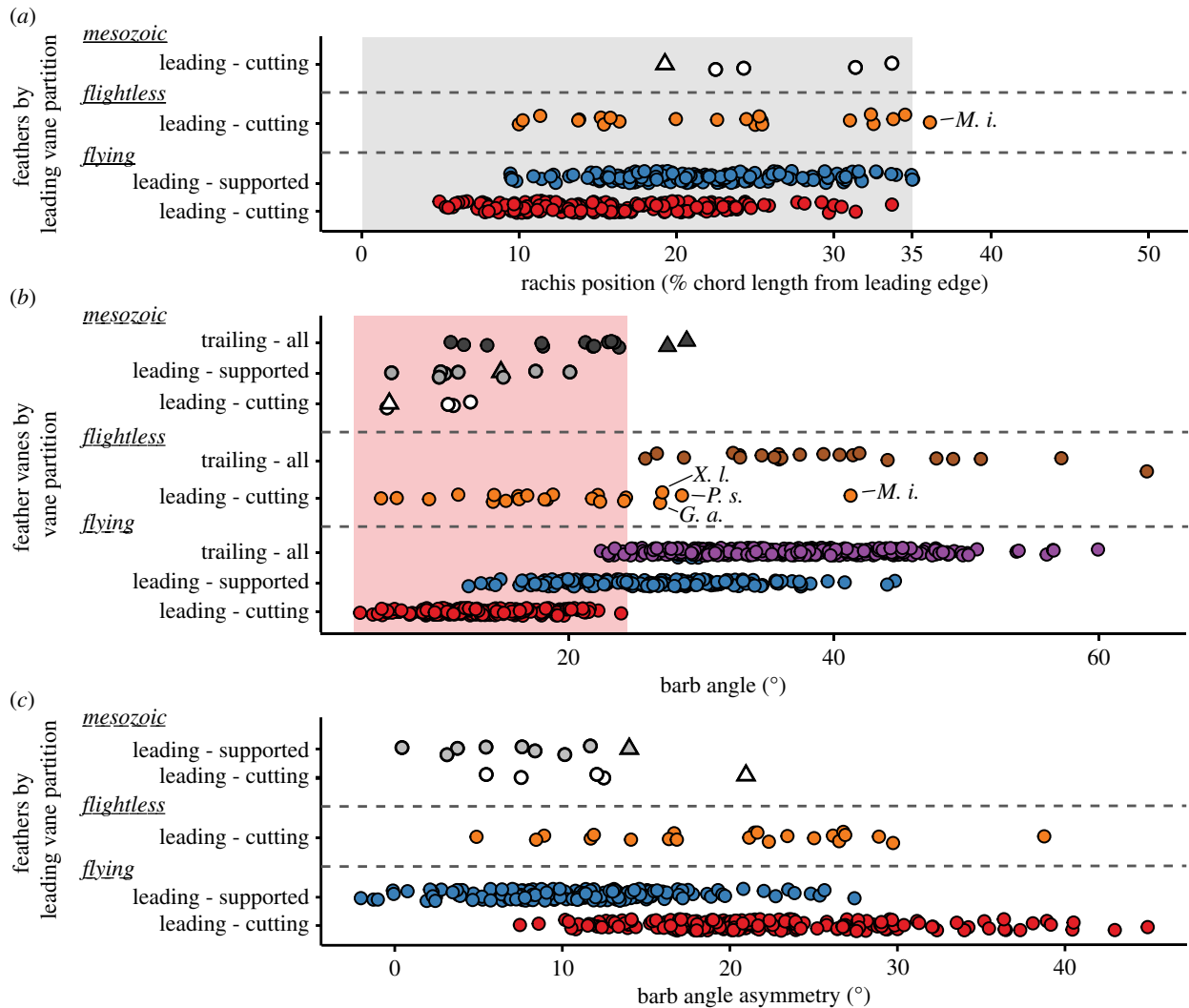


Figure 4. Flight feather vane asymmetry, barb angle and barb angle asymmetry of flying birds, flightless birds and Mesozoic stem birds. (a) Vane-width asymmetry was sufficient in all flight feathers of both stem and crown birds to position the rachis within the critical 35% limit for pitch control (grey box), except for the extant flightless rail *M. inepta*. (b) Leading vane barb angles of flightless crown birds (orange circles) and Mesozoic stem birds (white and grey shapes) fell within the range of flying cutting-edge vanes (red shading) except for the flightless *M. inepta*, *Po. sandwichensis*, *X. lyalli* and *G. australis* (orange circles outside of red shading). Among Mesozoic stem birds, only the enantiornithine *E. martini* (triangles) exhibited large trailing vane barb angles (black triangle), comparable with the modern bird condition (purple circles). Trailing vane barb angles of all other Mesozoic taxa (black circles) were relatively small compared with modern birds (purple circles). (c) Barb angle asymmetry in *E. martini* (triangles) was comparable with that of modern birds (blue and red circles), and was relatively low in stemward Mesozoic taxa (grey and white circles). (Online version in colour.)

the extent to which the underlying barb geometry of these feathers resembles those of modern birds has never been investigated. Vane-width asymmetry was sufficient in all Mesozoic flight feathers to position the rachis within the 35% functional threshold for automatic pitch control (figure 4a, white shapes). Barb angles of cutting-edge leading vanes of all Mesozoic stem birds were small (6–13°), falling well within the range of angles found in cutting-edge leading vanes of modern flying birds (figure 4b, white shapes versus red circles). By contrast, the barb angles of trailing vanes of early Mesozoic stem birds were small (11–24°), falling below the range of angles found in trailing vanes of modern birds (figure 4b, black circles versus purple circles). As a result, barb angle asymmetry in these early Mesozoic flight feathers was relatively low compared with modern birds (figure 4c, white and grey circles versus red and blue circles). Only the enantiornithine *E. martini*, the most crownward Mesozoic taxon in the analysis (figure 1), exhibited relatively large and comparably modern trailing vane barb angles (figure 4b, black triangles versus

purple circles), and a correspondingly modern degree of barb angle asymmetry (figure 4c, triangles).

4. Discussion

(a) Modern flying birds

Our survey of modern birds demonstrates that flight feather vane-width asymmetry is primarily determined by barb length. Contrary to previous assumptions [2,17,19,20], variation in barb angle is not related to variation in vane width or vane-width asymmetry, and instead varies with respect to the specific aerodynamic function of that portion of the feather vane (figure 3a,b). Barb angles are only small in leading vanes that function as the cutting edge of a feather or of an entire wing during flight, regardless of leading vane width. Supported leading vanes and trailing vanes have relatively large barb angles regardless of their vane width, or the degree of vane-width asymmetry.

Our results suggest that, within modern birds, variation in barb angle among different parts of the feather determines vane rigidity [19], whereas variation in barb length determines vane shape. This suggests that selection on aerodynamic function has taken advantage of the developmental independence of barb angle and barb length to adjust vane rigidity independently of changes in vane asymmetry for feather pitch stability, and changes in vane emarginations for drag reduction. In the case of flight feathers, the capacity of a cutting-edge vane to withstand aerodynamic forces as it cuts into the air is independent of the aerodynamic functions determined by the shape of the feather as a whole. The portions of leading vanes that function as a cutting edge within the wing occupy a distinct region of vane-width morphospace characterized by small barb angles (figure 2*d*). This pattern holds across a phylogenetic and functionally diverse sample of modern flying birds, suggesting that small barb angles in cutting-edge vanes, and the aerodynamic stability they confer, is a fundamental aerodynamic adaptation of avian flight.

Some leading vanes categorized as 'supported' in our study had small barb angles that fell within the range of cutting-edge vanes (figure 2*d*, blue squares with barb angles less than 24°). These feathers were all highly asymmetrical, and belonged to smaller species such as warblers, sparrows, and todies. In some taxa, highly asymmetrical primaries are known to separate during the upstroke owing to 'in-follicle' feather rotation, allowing leading vanes that overlap neighbouring feathers in a static spread wing to function as a cutting edge during the dynamic flight stroke [7]. Feather rotation in these instances is additionally facilitated by a curved rachis, as well as modifications to the attachments between the feather and the hand [7]. Although the distribution of feather rotation across extant birds has not been investigated, we hypothesize that the overlap in morphospace between our sample of cutting-edge leading vanes and some supported leading vanes reflects the misclassification of what appear to be 'supported' leading vanes in a spread wing that actually dynamically function as a cutting edge of the feather due to feather rotation during the upstroke.

(b) Modern flightless birds

Our survey of modern, secondarily flightless birds found that the primaries of most flightless birds are similar to modern flying birds in terms of their vane asymmetry and barb geometry. Congruent with the findings of several previous studies [30,31,34], most secondarily flightless species in our survey still retain functionally asymmetric primaries. This is in contrast to the conclusions drawn by Speakman & Thomson [8] in which they found the primaries of flightless birds to be significantly less asymmetrical than those of flying birds, but this discrepancy could be due to differences in taxon sampling between their study and the present one. Similarities in primary feather barb geometry between flying and flightless birds support the conclusions of Livezey [31,34], that the observed 'looseness' or reduced rigidity in the vanes of flightless taxa is primarily caused by degradation in the microstructure of their interlocking feather barbules.

(c) Mesozoic stem birds

The elongated wing feathers of Mesozoic Paraves exhibit small barb angles in cutting-edge leading vanes that are comparable with those of modern flying birds (figure 4*b*). This

suggests that the leading vanes of these Mesozoic feathers are functionally similar to those of modern birds, and were similarly capable of withstanding aerodynamic forces in airflow. Furthermore, our observations document that the outer hindwing feathers of the four-winged dromaeosaurid *Microraptor* were similar in vane structure to the primary feathers of two-winged Mesozoic taxa, corroborating previous interpretations of their aerodynamic function [33]. The presence of small cutting-edge barb angles, in conjunction with sufficient vane asymmetry for feather pitch stability, support the conclusion that some form of aerial locomotion was plesiomorphic for the most exclusive clade including *Microraptor* and modern birds (figure 1) [33].

Although the barb geometry of cutting-edge leading vanes in Mesozoic stem birds is essentially modern, barb geometry throughout the remaining portions of the early Mesozoic flight feather and wing are quantitatively distinct from those of modern birds. Unlike in modern birds, barb angles were relatively small in the trailing vanes of early Mesozoic stem birds (figure 4*b*). Only the enantiornithine *E. martini*, the most crownward Mesozoic paravian examined here, exhibits supported vane barb geometry that is comparable with modern birds. Larger barb angles in the trailing vanes evolved subsequent to the origin of asymmetrical flight feathers and the origin of aerial locomotion. The asymmetrical flight feathers of the early Mesozoic stem birds investigated here represent a new transitional morphology exhibiting some, but not all, of the features of modern avian flight feathers. Fully modern asymmetrical flight feather morphology, combining large supported vane barb angles with small cutting-edge leading vane barb angles, evolved well after the origin of vane asymmetry in Paraves, at some point along the internode between the lineage leading to *Confuciusornis*, and the most recent common ancestor of Enantiornithes and Ornithurae (figure 1).

The absence of modern trailing vanes in the flight feathers of stemward paravians—*Microraptor*, *Archaeopteryx*, *Sapeornis* and *Confuciusornis*—raises questions about the function of the derived larger barb angles in the trailing and supported leading vanes of modern birds and enantiornithines (figure 1). Supported trailing vanes overlap with other feathers as the wing is spread in flight, and function to maintain the integrity of the wing through the action of friction barbules [2,15]. Friction barbules on the obverse surface of trailing vanes mechanically 'catch' the reverse surface of overlapping leading vanes to prevent separation of the feathers during the flight stroke [15]. Larger barb angles help increase the flexibility of a vane [19], and we hypothesize that this flexibility could help maintain feather–feather contact and a coherent wing surface during flight by preventing failure of the friction barbules. Wings used for powered flight would be under more strain to maintain a coherent aerofoil during the active downstroke than wings used as a passive aerofoil during gliding. If larger barb angles in supported vanes do contribute to wing function, this would imply that the flight feather vanes of early stem birds were less flexible, and potentially less capable of maintaining a coherent aerofoil, than those of modern birds.

Our comparative analysis of flight feather barb geometry in Mesozoic stem birds indicates that the modern capacity to independently differentiate barb angles between the leading and trailing vanes of a feather evolved substantially after the origin of asymmetrical feathers with an aerodynamic function. Barb angle variation within modern avian flight

feathers is largely determined by differential barb expansion as the feather unfurls from its tubular sheath [17]. Within the flight feathers of modern birds, there is little to no barb expansion in the cutting-edge portions of a vane, and a relatively large degree of barb expansion throughout the rest of the feather [17]. The developmental processes that control barb expansion within a feather are largely unknown. Nevertheless, the developmental capacity for fine, differential control of barb angle expansion within a feather is integral to the acquisition of an aerodynamically modern flight feather. The absence of large trailing vane barb angles in early Mesozoic stem birds suggests that they lacked the capacity to differentially control barb angle. Ultimately, the ancestors of modern birds and enantiornithines evolved the developmental capacity to differentially control barb angle within the vanes of a single feather, allowing natural selection to refine the form of flight feathers for improved aerodynamic function.

Much of the debate surrounding the evolution of avian flight has focused on whether Mesozoic stem birds engaged solely in gliding, or in powered, flapping flight [12,35,36]. Since vane asymmetry and cutting-edge barb geometry would be advantageous features for any feathers that function as an aerofoil within airflow, the presence of these two characters in Mesozoic wing feathers suggest that stem birds were capable of some form of aerial locomotion from at least the Late Jurassic. However, these two characteristics in themselves do not provide specific evidence of either passive gliding or active, powered flight in early stem birds. Our data demonstrate that the entirely modern flight feather morphology (with small cutting-edge and large trailing vane barb angles) evolved along the internode separating *Confuciusornis* and the Enantiornithes + Ornithurae clade (figure 1). This finding implies that enantiornithines shared derived aerodynamic similarities in their flight stroke with modern birds that earlier stem birds lacked. The presence of the plesiomorphic Mesozoic flight feather morphology (small cutting-edge and small trailing vane barb angles) on the hindlimbs of *Microraptor* indicates that this feather morphology was functionally associated with passive gliding, at least in that taxon, because it is unlikely that *Microraptor* 'hindwings' functioned with a flapping flight stroke [33]. The observation that this plesiomorphic morphology is shared with *Archaeopteryx*, *Confuciusornis* and *Sapeornis*, raises the prospect that aerial locomotion in these taxa also consisted primarily of passive gliding. Although decisive conclusions regarding the aerial capacity

of these taxa awaits the integration of data from feather biomechanics, aerodynamic simulations and skeletal correlates, our data are congruent with the idea that Mesozoic paravians stemward of Enantiornithes may have been incapable of fully modern high-powered flight [12,35–38].

Our results document two stages in the evolution of modern flight feather morphology, illustrating a previously undocumented transitional morphology during the early evolution of avian flight [1,39]. The origin of the modern flight feather—characterized by small barb angles in cutting-edge vanes and larger barb angles in trailing vanes—is coincident with the inferred origin of multiple flight-related features, such as the alula and an ossified sternal keel [40,41]. These features arose subsequent to the origin of other hypothesized flight-related specializations such as the elongation of the coracoid, the acquisition of a fused pygostyle and the initial acquisition of asymmetrical flight feathers themselves [4]. Thus, the gradual, stepwise evolution of modern avian flight feathers parallels a broader, protracted period of flight apparatus refinement along the avian stem [1,39]. Although the precise phylogenetic origin of modern powered flying ability will continue to be debated, resolving this persistent controversy will depend on detailed comparative investigations of the components of the avian flight apparatus, incorporating both relevant fossil paravians as well as a broad phylogenetic sample of crown birds. This study brings us closer than ever before to a more complete understanding of the origin of modern asymmetrical flight feathers—one of the pre-eminent innovations in avian evolutionary history.

Data accessibility. Datasets related to this paper are available from Dryad (doi:10.5061/dryad.7vb83).

Acknowledgements. We thank P. Trail, A. Engilis, I. Engilis, K. Zyskowski, L. Garetano, P. Sweet, L. Chiappe, J. O'Connor, D. Schwartz-Wings, M. Ellison, M. Norell and S. Abramowicz for providing access to modern and fossil feather samples. L. Bonneau and P. Sweeney provided access to imaging equipment. K. Alexander assisted with feather scans, and E. Forrester provided guidance with phylogenetic comparative methods.

Author contributions. T.J.F., D.J.F. and R.O.P. designed the study. T.J.F. collected and analysed data and prepared figures. T.J.F., D.J.F. and R.O.P. wrote the manuscript.

Funding statement. T.J.F. was supported by the National Science Foundation Graduate Research Fellowship Program under grant no. DGE-1122492, and the Yale EEB Chair's Fund. D.J.F. was supported by an NSERC CGS-D and a Smithsonian Predoctoral Fellowship.

Conflict of interest. We have no competing interests.

References

- Makovicky PJ, Zanno LE. 2011 Theropod diversity and the refinement of avian characteristics. In *Living dinosaurs: the evolutionary history of modern birds* (eds G Dyke, GW Kaiser), pp. 10–29. Oxford, UK: John Wiley & Sons, Ltd.
- Lucas AM, Stettenheim PR. 1972 *Avian anatomy: integument*. *Agricultural handbook* 362. Washington, DC: US Dept. Agriculture.
- Prum RO, Brush AH. 2002 The evolutionary origin and diversification of feathers. *Q. Rev. Biol.* **77**, 261–295. (doi:10.1086/341993)
- Turner AH, Makovicky PJ, Norell MA. 2012 A review of dromaeosaurid systematics and paravian phylogeny. *Bull. Am. Mus. Nat. Hist.* **371**, 1–206. (doi:10.1206/748.1)
- Clarke JA. 2013 Feathers before flight. *Science* **340**, 690–692. (doi:10.1126/science.1235463)
- Feduccia A, Tordoff H. 1979 Feathers of *Archaeopteryx*: asymmetric vanes indicate aerodynamic function. *Science* **203**, 1021. (doi:10.1126/science.203.4384.1021)
- Norberg RÅ. 1985 Function of vane asymmetry and shaft curvature in bird flight feathers: inferences on flight ability of *Archaeopteryx*. In *The beginnings of birds* (eds MK Hecht, JH Ostrom, G Violh, P Wellnhofer), pp. 303–318. Eichstatt, Germany: Freunde des Jura-Museums.
- Speakman J, Thomson S. 1994 Flight capabilities of *Archaeopteryx*. *Nature* **370**, 514. (doi:10.1038/370514a0)
- Norberg RÅ. 1995 *Feather asymmetry in Archaeopteryx*. *Nature* **374**, 221–222.
- Longrich N. 2006 Structure and function of hindlimb feathers in *Archaeopteryx lithographica*. *Paleobiology* **32**, 417. (doi:10.1666/04014.1)
- Nudds RL. 2014 Reassessment of the wing feathers of *Archaeopteryx lithographica* suggests no robust evidence for the presence of elongated dorsal wing coverts. *PLoS ONE* **9**, e93963. (doi:10.1371/journal.pone.0093963)

12. Nudds RL, Dyke GJ. 2010 Narrow primary feather rachises in *Confuciusornis* and *Archaeopteryx* suggest poor flight ability. *Science* **328**, 887–889. (doi:10.1126/science.1188895)
13. Nudds RL, Dyke GJ. 2010 Response to comments on 'Narrow primary feather rachises in *Confuciusornis* and *Archaeopteryx* suggest poor flight ability'. *Science* **330**, 320. (doi:10.1126/science.1193474)
14. Foth C, Tischlinger H, Rauhut O. 2014 New specimen of *Archaeopteryx* provides insights into the evolution of pennaceous feathers. *Nature* **511**, 79–82. (doi:10.1038/nature13467)
15. Graham RR. 1932 Safety devices in wings of birds. *J. R. Aeronaut. Soc.* **36**, 24–58.
16. Tucker V. 1995 Drag reduction by wing tip slots in a gliding Harris' hawk, *Parabuteo unicinctus*. *J. Exp. Biol.* **198**, 775–781.
17. Feo TJ, Prum RO. 2014 Theoretical morphology and development of flight feather vane asymmetry with experimental tests in parrots. *J. Exp. Zool. (Mol. Dev. Evol.)* **322**, 240–255. (doi:10.1002/jez.b.22573)
18. Prum RO, Williamson S. 2001 Theory of the growth and evolution of feather shape. *J. Exp. Zool. (Mol. Dev. Evol.)* **291**, 30–57. (doi:10.1002/jez.4)
19. Ennos A, Hickson J, Roberts A. 1995 Functional morphology of the vanes of the flight feathers of the pigeon *Columba livia*. *J. Exp. Biol.* **198**, 1219.
20. Chandler AC. 1914 Modifications and adaptations to function in the feathers of *Circus hudsonius*. *Univ. Calif. Publ. Zool.* **11**, 329–376.
21. Schnute JT, Boers N, Haigh R, Grandin M, Johnson A, Wessel P, Antonio F. 2013 PBSmapping: mapping fisheries data and spatial analysis tools. R package version 2.66.53. See <http://CRAN.R-project.org/package=PBSmapping>.
22. Maddison WP, Maddison DR. 2011 *MESQUITE 2.75: a modular system for evolutionary analysis*, 2nd edn. See <http://medquiteproject.org>.
23. Jetz W, Thomas G, Joy J, Hartmann K, Mooers AO. 2012 The global diversity of birds in space and time. *Nature* **491**, 444–448. (doi:10.1038/nature11631)
24. R Core Team. 2014 *R: a language and environment for statistical computing*. Vienna, Austria: R Foundation for Statistical Computing.
25. Paradis E, Claude J, Strimmer K. 2004 APE: analyses of phylogenetics and evolution in R language. *Bioinformatics* **20**, 289–290. (doi:10.1093/bioinformatics/btg412)
26. Orme D. 2013 The caper package: comparative analysis of phylogenetics and evolution in R.
27. Dunning JB. 1993 *CRC handbook of avian body masses*. Boca Raton, FL: CRC.
28. Bruderer B, Peter D, Boldt A, Liechti F. 2010 Wing-beat characteristics of birds recorded with tracking radar and cine camera. *Ibis* **152**, 272–291. (doi:10.1111/j.1474-919X.2010.01014.x)
29. Field DJ, Lynner C, Brown C, Darroch SAF. 2013 Skeletal correlates for body mass estimation in modern and fossil flying birds. *PLoS ONE* **8**, e82000. (doi:10.1371/journal.pone.0082000)
30. McGowan C. 1989 Feather structure in flightless birds and its bearing on the question of the origin of feathers. *J. Zool.* **218**, 537–547. (doi:10.1111/j.1469-7998.1989.tb04997.x)
31. Livezey BC. 2003 Evolution of flightlessness in rails (Gruiformes, Rallidae). *Ornithol. Monogr.* **53**, 1–654.
32. Livezey BC, Humphrey PS. 1986 Flightlessness in steamer-ducks (Anatidae: *Tachyeres*): its morphological bases and probable evolution. *Evolution* **40**, 540. (doi:10.2307/2408576)
33. Xu X, Zhou Z, Wang X, Kuang X, Zhang F, Du X. 2003 Four-winged dinosaurs from China. *Nature* **421**, 335–340. (doi:10.1038/nature01342)
34. Livezey BC. 1992 Morphological corollaries and ecological implications of flightlessness in the kakapo (Psittaciformes: *Strigops habroptilus*). *J. Morphol.* **213**, 105–145. (doi:10.1002/jmor.1052130108)
35. Vazquez RJ. 1992 Functional osteology of the avian wrist and the evolution of flapping flight. *J. Morphol.* **211**, 259–268. (doi:10.1002/jmor.1052110303)
36. Senter P. 2006 Scapular orientation in theropods and basal birds, and the origin of flapping flight. *Acta Palaeontol. Pol.* **51**, 305–313.
37. Allen V, Bates KT, Li Z, Hutchinson JR. 2013 Linking the evolution of body shape and locomotor biomechanics in bird-line archosaurs. *Nature* **497**, 104–107. (doi:10.1038/nature12059)
38. Field DJ, Lynner C. 2013 Precise inference of avialan flight ability from shoulder joint dimensions. *J. Vert. Paleontol.* Program and abstracts, p. 126.
39. Clarke JA, Middleton KM. 2008 Mosaicism, modules, and the evolution of birds: results from a Bayesian approach to the study of morphological evolution using discrete character data. *Syst. Biol.* **57**, 185–201. (doi:10.1080/10635150802022231)
40. Sanz JL, Chiappe LM, PerezMoreno BP, Buscalioni AD, Moratalla JJ, Ortega F, PoyatoAriza FJ. 1996 An Early Cretaceous bird from Spain and its implications for the evolution of avian flight. *Nature* **382**, 442–445. (doi:10.1038/382442a0)
41. Zheng X, Wang X, O'connor J, Zhou Z. 2012 Insight into the early evolution of the avian sternum from juvenile enantiornithines. *Nat. Commun.* **3**, 1116. (doi:10.1038/ncomms2104)